Fermi National Accelerator Laboratory

FERMILAB-Conf-97/346-E
D0

QCD Results from D0

Nikos Varelas
For the D0 Collaboration

Michigan State University
East Lansing, Michigan 48824
and *Univeristy of Illinois at Chicago*
Chicago, Illinois 60607

Fermi National Accelerator Laboratory
P.O. Box 500, Batavia, Illinois 60510

October 1997

Published Proceedings of the *High Energy Physics International Euroconference on QCD*, Montpellier, France, July 3-9, 1997

Operated by Universities Research Association Inc. under Contract No. DE-AC02-76CH03000 with the United States Department of Energy

QCD Results from DØ

Nikos Varelas[a]*

[a] Michigan State University, East Lansing, Michigan 48824, USA
and
University of Illinois at Chicago, Chicago, IL 60607, USA

We present recent results on jet production, dijet angular distributions, $W+$ Jets, and color coherence from $p\overline{p}$ collisions at $\sqrt{s} = 1.8$ TeV at the Fermilab Tevatron Collider using the DØ detector. The data are compared to perturbative QCD calculations or to predictions of parton shower based Monte Carlo models.

1. INTRODUCTION

The Tevatron Collider provides a unique opportunity to study the properties of hard interactions in $p\overline{p}$ collisions at short distances. Colored partons from a hard scatter evolve via soft quark and gluon radiation and hadronization processes to form observable colorless hadrons, which appear in the detector as localized energy deposits identified as jets. Jet detection in DØ relies primarily on the excellent linearity and fine transverse and longitudinal segmentation of the uranium–liquid argon calorimeters [1]. It has hermetic coverage for pseudorapidity $|\eta| < 4$ ($\eta = -\ln[\tan(\theta/2)]$, where θ is the polar angle of the jet with respect to the proton beam) with fractional transverse energy E_T resolution of $\sim 80\%/\sqrt{E_T(\mathrm{GeV})}$ for jets.

Jets were reconstructed offline using an iterative jet cone algorithm with a cone radius $R = \sqrt{(\Delta\eta)^2 + (\Delta\phi)^2} = 0.7$. Spurious jets from isolated noisy calorimeter cells and accelerator losses were eliminated by loose cuts on the jet shape. The E_T of each jet was corrected for offsets due to the underlying event, multiple $p\overline{p}$ interactions, and noise; out–of–cone showering; and detector energy response as determined from the missing transverse energy balance of photon–jets events.

This report presents recent results on jet production, dijet angular distributions, $W+$ Jets, and color coherence from the DØ experiment. The data sample was collected during the 1994–1995 Tevatron Collider run and represents an integrated luminosity of 93 pb^{-1}.

2. HIGH-E_T JET RESULTS

The production of jets at large E_T and its comparison with perturbative QCD calculations are of interest as they can serve to test the extend to which partons are elementary. The measurement of the inclusive jet cross section at the Tevatron has been followed with great interest since the report of excess events at large transverse energies by the CDF Collaboration [2].

The DØ Collaboration has measured jet cross sections over eight orders of magnitude in $d^2\sigma/dE_T d\eta$ up to $E_T = 500$ GeV, halfway to the kinematic limit. The challenge in measuring such a steeply falling spectrum is the understanding of the energy calibration of jets. The highest E_T jets are not directly calibrated, resulting in large uncertainties. In this kinematic region the next–to–leading order (NLO) calculations are well understood at the 10–20% level. However, precise knowledge of the parton distribution functions (pdf's) in the proton is required before firm conclusions can be drawn from the comparison of data and theory. Collider data can constrain the parton distribution functions in the proton and especially the gluon distribution at moderate x.

The DØ preliminary inclusive jet cross section measurement in the region $|\eta| \leq 0.5$ is shown in Fig. 1. The observed E_T spectrum has been corrected for resolution smearing by assuming a trial unsmeared spectrum, $(AE_T^{-B}) \cdot (1 - 2E_T/\sqrt{s})^C$,

*For the DØ Collaboration

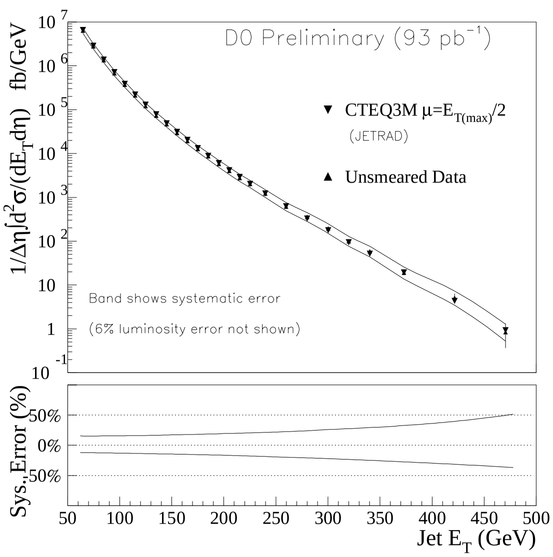

Figure 1. A comparison of the DØ central inclusive jet cross section to a NLO QCD calculation. The points include statistical errors. The inset curves represent $\pm$ 1 σ systematic uncertainty.

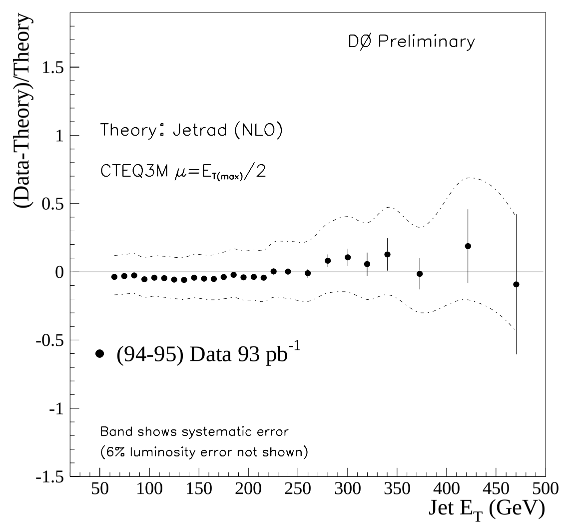

Figure 2. Difference between the inclusive jet cross section as measured by DØ and NLO QCD normalized to the theoretical prediction.

and fitting its convolution with the measured resolution to the measured cross section. The data are plotted with their (uncorrelated) statistical errors; in addition, there is an overall luminosity uncertainty of 6%. The inset shows the total systematic uncertainty (without the luminosity uncertainty) as a function of E_T. It is dominated by the jet energy scale uncertainty.

Figure 1 also shows a prediction of the inclusive jet cross section from the NLO parton event generator JETRAD [3]. The NLO calculation requires specification of the renormalization and factorization scale ($\mu = E_T^{\max}/2$ where $E_T^{\max}$ is the maximum jet E_T in the generated event), pdf (CTEQ3M [4]), and the parton clustering algorithm. Partons within $1.3\times\mathcal{R}$ of one another were clustered if they were also within $\mathcal{R}$=0.7 of their E_T weighted η, ϕ centroid. The value of $1.3\times\mathcal{R}$ was determined by overlaying jets from separate events and determining the separation at which the jet reconstruction algorithm could resolve the individual jets [5].

Figure 2 shows the ratio, $(D-T)/T$, for the data (D) and NLO theoretical (T) predictions. The NLO predictions are in excellent agreement with the data in shape and normalization.

The dijet angular distribution is an ideal tool to examine signatures of new physics in events with high$-E_T$ jets. The angular distribution of the outgoing partons is strictly governed by the helicities of the partons participating in the hard process and is relatively insensitive to the parton densities. Any unusual contact interaction (with effective scale Λ) will flatten the center of mass scattering angle distribution. The CDF Collaboration has recently published results on dijet angular distributions that give a lower limit of $\Lambda > 1.8$ TeV [6].

The dijet angular distribution is typically expressed in term of χ, where $\chi = (1+\cos\theta^*)/(1-\cos\theta^*) = e^{|\eta_1-\eta_2|}$. This is done in order to flatten out the t-channel pole contribution to the distribution and to facilitate an easier comparison to the predictions of QCD. It also allows signatures of new physics that might have a more isotropic angular distribution than QCD (e.g., quark compositeness) to be more easily examined as they

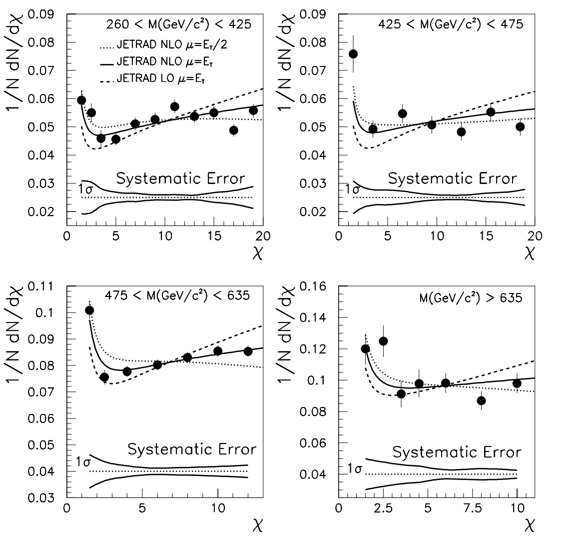

Figure 3. Dijet angular distributions for DØ data compared to JETRAD for LO and NLO predictions with two different renormalization/factorization scales.

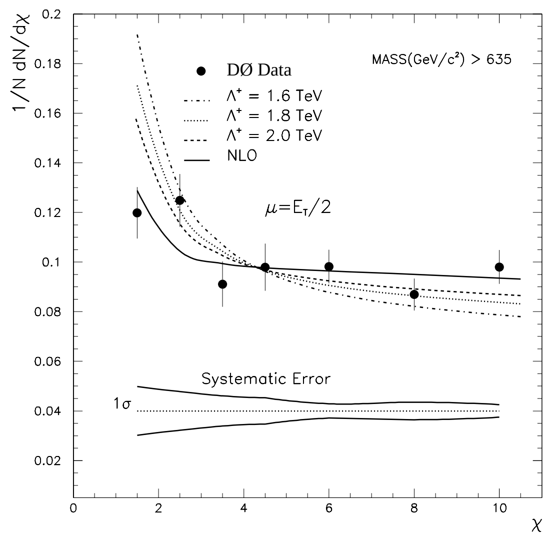

Figure 4. Dijet angular distributions for DØ data compared to theory for different compositeness scales. See text for how compositeness is calculated for NLO predictions. The errors on the points are statistical and the band represents the correlated $\pm$ 1 σ systematic uncertainty.

would produce an excess at low values of χ.

The quantity measured in the dijet angular analysis is $1/N(dN/d\chi)$, for four ranges of the dijet mass. The two leading–E_T jets were required to have a maximum pseudorapidity less than 3.0. For the mass bins and χ values presented, a cut on $|\eta_{\rm boost}| = \frac{1}{2}|(\eta_1 + \eta_2)| < 1.5$ was applied to ensure uniform acceptance.

Figure 3 shows the DØ χ distributions [7] normalized to unit area compared to three different theoretical predictions. The QCD predictions are clearly sensitive to the order of the calculation and to the renormalization scale. The NLO predictions are seen to be in better agreement with the data than the LO calculations, especially for large χ.

Because the currently available NLO calculations do not implement the effects of both QCD and quark substructure, possible effects of quark compositeness are determined using a LO simulation [8]. The ratio of the LO predictions with compositeness to the LO predictions with no compositeness is used to scale the NLO calculation. Figure 4 shows the dijet angular distribution for events with $M > 635$ GeV/c^2 compared to theory for different values of the compositeness scale, Λ^+. The largest dijet invariant mass bin is shown because the effects of quark compositeness become more pronounced with increasing dijet invariant mass. To obtain a compositeness limit, we constructed the variable R_χ, the ratio of the number of events with $\chi < 4$ to the number of events with $4 < \chi < \chi_{\rm max}$. Using these data, DØ rules out at 95% CL a model where quarks couple with a universal contact interaction of scale $\Lambda \sim 2.1$ TeV, varying slightly with the choice of renormalization/factorization scale and details of the compositeness model.

3. $W+$ JETS PRODUCTION

Hadronic production of W bosons provides an important test of perturbative QCD calculations.

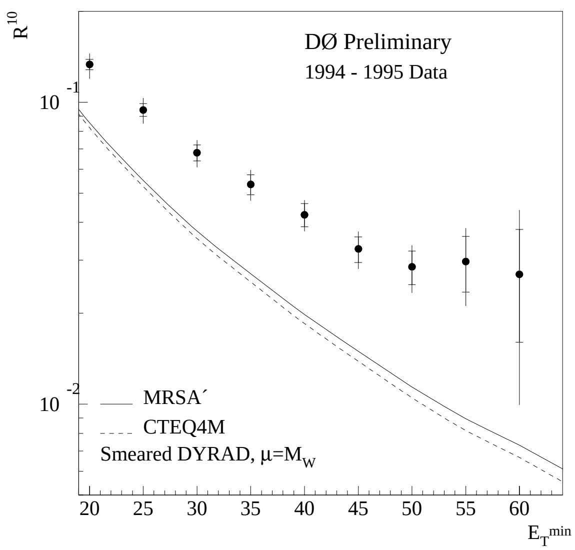

Figure 5. The DØ $(W+1$ Jet$)$ $/(W+0$ Jets$)$ as a function of jet E_T^{min} compared to the smeared DYRAD predictions using CTEQ4M and MRSA' pdf's.

The UA1 and UA2 experiments [9,10] used events with a W boson and jets to measure the ratio, $\mathcal{R}^{10}$, of the production cross section for $W+1$ Jet events relative to that for $W+0$ Jets events and then used theoretical calculations to extract a value for the strong coupling constant at the mass of the W, $\alpha_S(M_W^2)$. The DØ Collaboration has also published [11] a measurement of the ratio of production cross sections using the data from the 1992–1993 run of the Tevatron Collider. The preliminary results presented here are from the high statistics 1994–1995 run (six times larger data set).

Events with the decay $W \to e+\nu$ events were used and required to have an isolated electron with $E_T > 25$ GeV, and $|\eta| < 1.0$. The events were required to have missing transverse energy $\not\!\!E_T >$ 25 GeV. The dependence of the ratio on the minimum jet E_T, E_T^{min}, is compared to NLO QCD predictions. The data sample consists of 36,984 events with 32,879 $W+0$ Jets and 2,574 $W+1$ Jet events for $E_T^{min} = 25$ GeV.

The dominant source of background to $W+$ Jets events comes from multijet events in which one jet fluctuated highly electromagnetically and another jet was mismeasured to produce substantial $\not\!\!E_T$. The amount of background from this source for the $W+0$ Jets and $W+1$ Jet samples was studied as a function of $\not\!\!E_T$ by comparison with an unbiased trigger sample. Additional backgrounds were estimated using the ISAJET Monte Carlo.

Energy calibration corrections were applied to the electrons and jets. Differences in the electron selection efficiencies as a function of jet multiplicity were also taken into account. The jet energy corrections and the electron efficiency corrections both introduce a systematic error of $\pm 5\%$ on the ratio for $E_T^{min} = 25$ GeV.

In Fig. 5 the $\mathcal{R}^{10}$ ratio is plotted for both data and theory as a function of jet E_T^{min}. The NLO theory was calculated using DYRAD [12] with various pdf's from the MRSA' [13] and CTEQ4 [14] families using a renormalization/factorization scale of M_W. There is a slight normalization difference between the predictions with the different pdf's, but they are both well below the data.

Figure 6 shows the ratio for E_T^{min}= 25 GeV with theory predictions made for different values of α_S. The lines and shaded band represent the measurement. The solid line is the experimental result. The dotted lines indicate the statistical errors only while the shaded region indicates the statistical and systematic errors added in quadrature. The points are the predictions using both the CTEQ4 family and the MRSA family of pdf's. The lack of dependence on α_S in the predictions can be attributed to cancellations between the matrix elements and the gluon distribution as α_S is varied.

We note that the W p_T can be much smaller than the E_T^{min} due to the effects of extra jets and unclustered E_T. This effect appears particularly in the data.

4. COLOR COHERENCE EFFECTS IN $W+$ JETS EVENTS

In perturbative QCD, color coherence effects arise from interference of soft gluon radiation

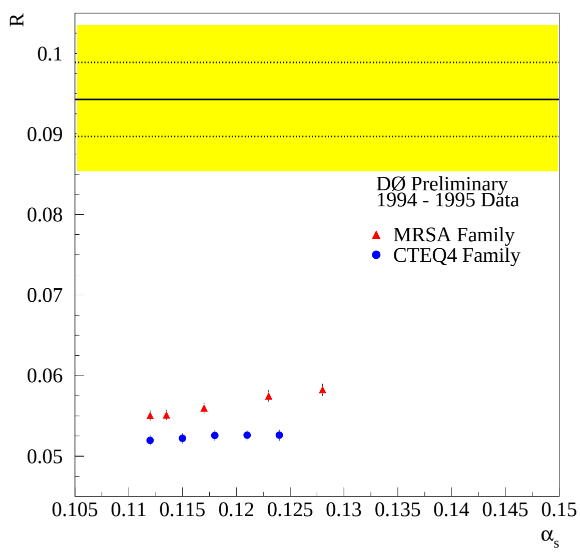

Figure 6. The DØ ($W+1$ Jet) /($W+0$ Jets) for E_T^{min}=25 GeV compared to the smeared DYRAD predictions as a function of α_S using CTEQ4M and MRSA pdf's. The dotted lines are the statistical errors on the measurement, while the shaded band is the systematic and statistical uncertainties added in quadrature.

emitted from color connected partons [15–17]. Color coherence, which results in a suppression of soft gluon radiation in the partonic cascade in certain regions of phase space, can be approximated by *Angular Ordering* (AO). In this approximation the successive emission angles of soft gluons decrease as the cascade evolves away from the hard process. For incoming partons the emission angles increase as the process evolves from the initial hadrons to the hard subprocess. Monte Carlo simulations including coherence effects probabilistically by means of AO are available for both initial and final state evolutions. In the nonperturbative regime, color coherence effects are modeled by phenomenological fragmentation models with results qualitatively similar to perturbative AO effects.

Color coherence effects in $p\overline{p}$ interactions have been previously studied [18,19] by measuring spatial correlations between soft and leading–E_T jets in multijet events. Here we report on a study of color coherence in $W+$ Jets events. This is the first observation of color coherence effects in $p\overline{p}$ events containing W bosons and jets.

In $W+$ Jets events, the angular distribution of soft gluons about the colorless W boson is expected to be uniform, while the distribution around the jet is expected to have structure due to the colored partons in the jet. These effects are studied by comparing the distributions of soft particles around the W boson and opposing jet directions. This comparison reduces the sensitivity to global detector and underlying event biases that may be present in the vicinity of the W boson and the jet.

Once the W boson direction has been determined in the detector, the opposing jet is identified by selecting the leading–E_T jet in the ϕ hemisphere opposite to the W boson. Annular regions are drawn around both the W boson and the jet in (η,ϕ) space. The angular distributions of towers ($\Delta\eta \times \Delta\phi = 0.1 \times 0.1$) above the 250 MeV threshold are measured in these annular regions using the polar variables $R = \sqrt{(\Delta\eta)^2 + (\Delta\phi)^2}$ and $\beta_{W,Jet} = \tan^{-1}(\frac{sign(\eta_{W,Jet})\cdot\Delta\phi_{W,Jet}}{\Delta\eta_{W,Jet}})$; where $\Delta\eta_{W,Jet} = \eta_{Tower} - \eta_{W,Jet}$ and $\Delta\phi_{W,Jet} = \phi_{Tower} - \phi_{W,Jet}$, in a search disk of $0.7 < R < 1.5$. Color coherence effects are expected to manifest themselves as a depletion in the energetic tower distribution around the tagged jet in the transverse plane relative to the event plane (when compared with the W boson distribution). In order to minimize the statistical uncertainties in the $W+$ Jets sample, the annuli are folded about the ϕ symmetry axis, thereby reducing the β range to 0–π.

We selected $W \rightarrow e+\nu$ events with at least one jet with $E_T > 10$ GeV. The event selection criteria include $E_T^e > 25$ GeV, $\not{E}_T > 25$ GeV, $p_T^W > 10$ GeV/c, $|\eta_{Jet}| < 0.7$, and W boson rapidity $|y_W| < 0.7$. Additionally, the z component of the event vertex was restricted to $|z_{vtx}| < 20$ cm to retain the projective nature of the calorimeter towers.

The data angular distributions are compared to three Monte Carlo samples, generated with different levels of color coherence effects, using

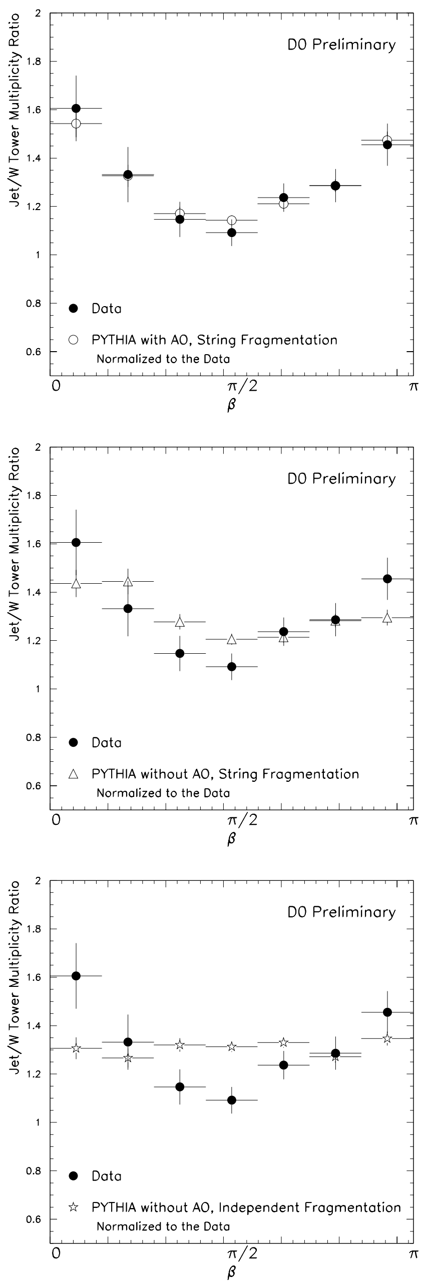

Figure 7. Comparison of the Jet/W tower multiplicity ratio between the DØ data (solid circles) and PYTHIA with various color coherence implementations. The Monte Carlo events have been normalized to the data.

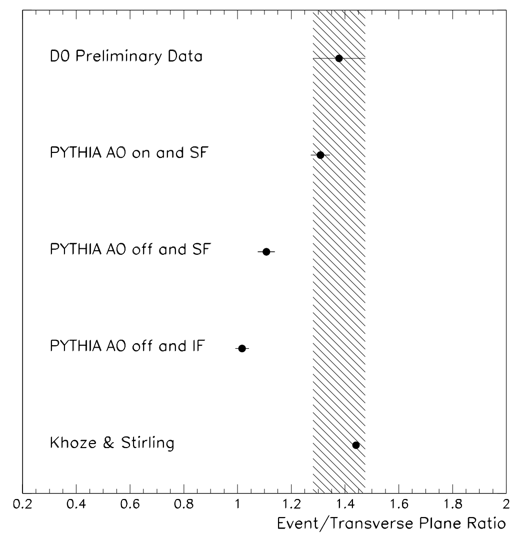

Figure 8. Ratio of event plane to transverse plane of Jet/W tower multiplicity for DØ data, PYTHIA with various color coherence implementations, and a MLLA QCD calculation. The errors are statistical only.

the PYTHIA 5.7 parton shower event generator [20] and passed through a full detector simulation. PYTHIA, with both AO and string fragmentation (SF) implemented, accounts for color coherence effects at both the perturbative and nonperturbative levels. Turning off AO removes the perturbative contribution, and using independent fragmentation (IF) eliminates the nonperturbative component. Finally, a comparison to a recent Modified Leading–Log Approximation (MLLA) perturbative calculation of Khoze and Stirling [21] based on the local parton–hadron duality hypothesis [15] is also presented.

Figure 7 shows the ratio of the tower multiplicity around the jet to the tower multiplicity around the W as a function of β. The number of towers is greater for the jet than for the W boson and the excess is enhanced in the event plane ($\beta = 0, \pi$) and minimized in the transverse plane ($\beta = \frac{\pi}{2}$), consistent with the expectation from initial–to–final state color interference effects. The errors include only statistical uncertainties, which are significantly larger than all systematic uncertainties considered. Also shown in Fig. 7 are the predictions from PYTHIA with various color coherence implementations. PYTHIA with AO and string fragmentation is in good agreement with the $W+$ Jets data. PYTHIA with AO off and string fragmentation agrees less well, and PYTHIA with AO off and independent fragmentation does not reproduce the data.

A measure of the observed color coherence effect is obtained by calculating the Jet/W tower multiplicity enhancement of the event plane ($\beta = 0, \pi$) to the transverse plane ($\beta = \pi/2$), which would be expected to be unity in the absence of color coherence effects. This ratio of ratios is insensitive to the overall normalization of the individual distributions, and Monte Carlo studies have shown that it is relatively insensitive to detector effects. Figure 8 compares the data to the various PYTHIA predictions. Again, we see good agreement with PYTHIA with AO on and string fragmentation, and disagreement with AO off and string fragmentation or AO off and independent fragmentation. The MLLA predictions by Khoze and Stirling are in a very good agreement with the data, giving additional evidence supporting the validity of the local parton–hadron duality hypothesis.

5. Conclusions

We have measured the central inclusive jet cross section and dijet angular distributions and found them to be in agreement with NLO QCD predictions. We have excluded a compositeness model where quarks couple with a universal left–handed contact interaction up to a scale $\Lambda \sim 2.1$ TeV. We have studied $W+$ Jets final states, and observed discrepancies between NLO QCD and our measurement of the production cross section for $W + 1$ Jet events relative to that for $W + 0$ Jets events. We have observed color coherence effects in $W+$ Jets events, and demonstrated that these effects survive the nonperturbative hadronization process. Our data are in agreement with PYTHIA predictions when both angular ordering and string fragmentation are included, and also with recent MLLA QCD calculations based on the local parton–hadron duality hypothesis.

6. Acknowledgments

We thank W.Giele, V. Khoze, T. Sjöstrand, and J. Stirling for valuable discussions. We thank the staffs at Fermilab and collaborating institutions for their contributions to this work, and acknowledge support from the Department of Energy and National Science Foundation (U.S.A.), Commissariat à L'Energie Atomique (France), State Committee for Science and Technology and Ministry for Atomic Energy (Russia), CNPq (Brazil), Departments of Atomic Energy and Science and Education (India), Colciencias (Colombia), CONACyT (Mexico), Ministry of Education and KOSEF (Korea), and CONICET and UBACyT (Argentina).

REFERENCES

1. DØ Collaboration, S. Abachi *et al.*, Nucl. Instrum. Meth. **A338**, 185 (1994).
2. CDF Collaboration, F. Abe *et al.*, Phys. Rev. Lett. **70**, 1376 (1993); Phys. Rev. Lett. **77**, 438 (1996).
3. W.T. Giele, E.W.N. Glover, and D.A. Kosower, Nucl. Phys. **B403**, 633 (1993); Phys. Rev. Lett. **73**, 2019 (1994).
4. CTEQ Collaboration, H.L. Lai *et al.*, Phys. Rev. D **51** 4763 (1995).
5. B. Abbott *et al.*, Fermilab-Pub-97/242-E, (unpublished).
6. CDF Collaboration, F. Abe *et al.*, Phys. Rev. Lett. **77**, 5336 (1996); Erratum - ibid. **78**, 4307 (1997).
7. DØ Collaboration, B. Abbott *et al.*, hep-ex/9707016, submitted to Phys. Rev. Lett.
8. E. Eichten, K. Lane, and M. Peskin, Phys. Rev. Lett. **50**, 811 (1983).
9. UA1 Collaboration, M. Lindgren *et al.*, Phys. Rev. D **45**, 3038 (1992).
10. UA2 Collaboration, J. Alitti *et al.*, Phys. Lett. B **263**, 563 (1991).
11. DØ Collaboration, S. Abachi *et al.*, Phys. Rev. Lett. **75**, 3226 (1995).

12. W.T. Giele, E.W.N. Glover, and D.A. Kosower, Nucl. Phys. B **403**, 633 (1993).
13. A. D. Martin *et al.*, Phys. Lett. B **356**, 89 (1995).
14. H. L. Lai *et al.*, Phys. Rev. D **55**, 1280 (1997).
15. Ya.I. Azimov, Yu.L. Dokshitzer, V.A. Khoze, and S.I. Troyan, Phys. Lett. **B165**, 147 (1985); Sov. Journ. Nucl. Phys. **43**, 95 (1986).
16. R.K. Ellis, G. Marchesini, and B.R. Webber, Nucl. Phys. **B286**, 643 (1987); Erratum Nucl. Phys. **B294**, 1180 (1987).
17. Yu.L. Dokshitzer, V.A. Khoze, A.H. Mueller, and S.I. Troyan, Basics of Perturbative QCD, Editions Frontières (1991); Rev. Mod. Phys. **60**, 373 (1988); Yu.L. Dokshitzer, V.A. Khoze, and S.I. Troyan, Sov. Journ. Nucl. Phys. **46**, 712 (1987).
18. CDF Collaboration, F. Abe *et al.*, Phys. Rev. **D50**, 5562 (1994).
19. DØ Collaboration, B. Abbott *et al.*, hep-ex/9706012, submitted for publication.
20. T. Sjöstrand, Computer Physics Commun. **82**, 74 (1994).
21. V. Khoze and J. Stirling, hep-ph/9612351.